



## OPTICAL PROBE CURRENT SENSOR MODULE USING THE KERR EFFECT OF EXCHANGE-COUPLED MAGNETIC FILM AND ITS APPLICATION TO IGBT SWITCHING CURRENT MEASUREMENTS

K. Ogawa<sup>1</sup>, S. Suzuki<sup>1</sup>, M. Sonehara<sup>1</sup>, T. Sato<sup>1</sup>, K. Asanuma<sup>2</sup>

<sup>1</sup>Spin Device Technology Center, Shinshu University

Nagano, Nagano, Japan 380-8553

Emails: [keisuke@yslab.shinshu-u.ac.jp](mailto:keisuke@yslab.shinshu-u.ac.jp)

<sup>2</sup>Department of Production Engineering

Nagano Prefectural Institute of Technology

Ueda, Nagano, Japan 386-1211

---

*Submitted: Mar. 31, 2012*

*Accepted: May 8, 2012*

*Published: June 1, 2012*

---

*Abstract- An optical probe current sensor module using the Kerr effect of exchange-coupled magnetic film has been fabricated and applied to switching current measurements for IGBT used for the DC-DC converter and the DC-AC inverter of EV/HEV. Since the sensor module using the Kerr effect of the single domain exchange-coupled magnetic film utilizes magnetization rotation only, Barkhausen noise due to domain wall pinning can be excluded. The current sensor consists of a Laser-diode, a polarizer, a Fe-Si/Mn-Ir exchange-coupled film, a quarter-wavelength plate, PIN Photodiodes and a differential*

*amplifier. The current sensor has a current measurement range of  $\pm 60$  A and a frequency range of DC-200 kHz. The switching current of IGBT has been measured by it.*

**Index terms:** Current sensor, Optical probe, Magneto-optical Kerr effect, Exchange-coupled film, EV/HEV

## I. INTRODUCTION

In order to reduce CO<sub>2</sub> emissions from vehicles, the electric vehicle (EV) and the hybrid electric vehicle (HEV) have been developed and they are increasing worldwide. To further increase their energy efficiency, higher efficient the Power Control Unit (PCU) with the DC-DC converter and the DC-AC inverter must be realized.

Fig. 1 shows an example of the PCU [1]. When the synchronous motor is driven by the inverter, it is necessary to measure the motor current correctly for torque control. Also for monitoring the charge/discharge energy of the battery, current sensor is needed. The Hall element sensor with a magnetic yoke is currently used for sensing the motor current and the charge/discharge current of the battery. However, it is not so easy to measure the current correctly because the electromagnetic noise, which is due to very large current switching in the PCU with a rating power of 10 – 100 kW, is induced in the wire-harness of the sensor, and such noise degrades S/N

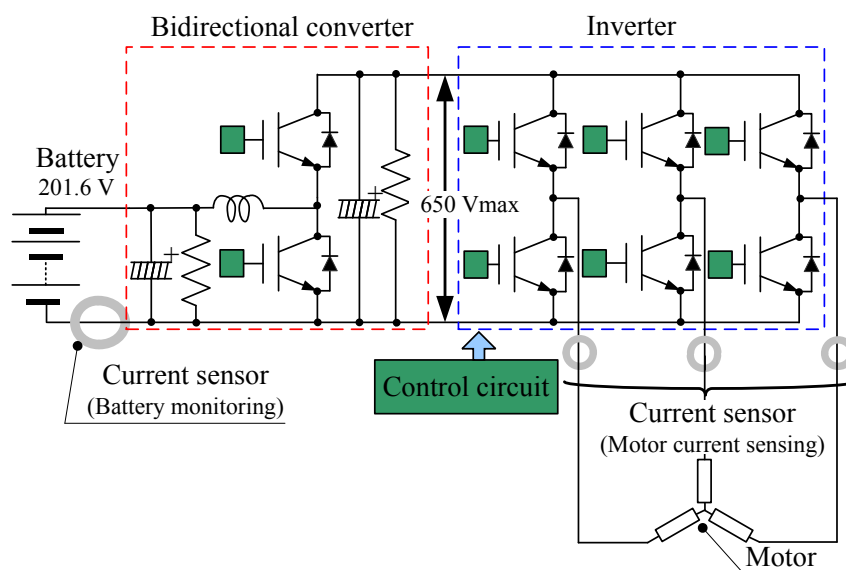


Fig.1 Power control unit of the Electric vehicle and the hybrid electric vehicle.

ratio of the current sensing [2]. In addition, the Hall-effect sensor has the undesired temperature dependent drift.

Optical probe sensing is effective for suppressing the influence of electromagnetic noise. As the previous optical probe sensing, optical current transformer [3], fiber-edge magneto-optic probe [4], [5] and others are well-known methods for current sensing or magnetic field sensing by using the magneto-optical Faraday-effect [6]. However, such conventional sensor systems have not been applied to EV/HEV current sensing owing to the temperature dependent characteristics of magneto-optic (MO) material such as Bi-RIG with low Curie temperature below 300 degree C.

The authors used the magneto-optical Kerr effect for current sensing. The Kerr-effect has been commonly used for evaluation of magnetic materials, such as magnetic domain observation [7]. By using the metallic magnetic film with high Curie temperature for Kerr-effect optical sensor, temperature dependence of the sensor characteristic can be improved.

In this study, a novel optical probe current-sensor module, based on the Kerr effect for rotation magnetization of the single magnetic-domain Fe-Si/Mn-Ir exchange-coupled film[8], has been fabricated and applied to switching current measurements for the IGBT used in the PCU. The accurate switching current sensing in the PCU is very important to realize the optimal switching control scheme (e.g., zero-current switching) for minimizing the switching-loss. Since the optical sensor signal is transmitted through the optical-fiber, the ambient EMI noise does not influence the sensor signal.

In this paper, we report on fabrication and evaluation of the optical probe current sensor module and its application to a switching current measurement for the IGBT used for the PCU of the EV/HEV.

## II. MAGNETIC KERR EFFECT AND ITS APPLICATION TO OPTICAL PROBE CURRENT SENSOR MODULE

### a. Current dependent Kerr rotation of a single magnetic-domain film

Fig.2 shows the Kerr effect and operation principle of the optical probe current sensor. A single magnetic-domain film is put on conductor line (a wire or a bus-bar, etc) to align a magnetic moment in the current flow direction. An incident plane of linearly polarized light is aligned in the hard magnetization direction of the magnetic film. When the current is zero, the transverse

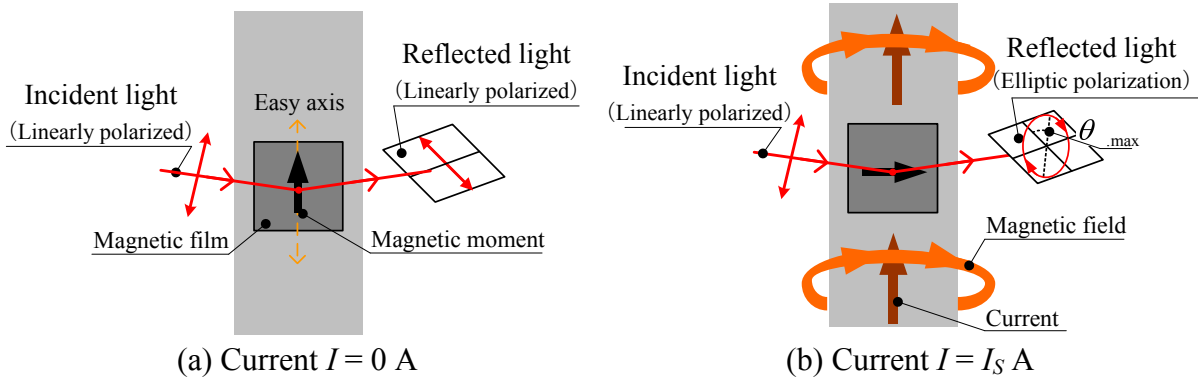


Fig. 2 Principle of the magnetic Kerr effect and the optical probe sensor.

Kerr effect becomes dominant and the reflected light is to be kept to the linear polarization. When the current  $I_s$  is flowing in the bus-line, which is large enough to align the magnetic moment perpendicular to the current direction, the reflected light is elliptically polarized with a maximum Kerr rotation  $\theta_{K,max}$ . In case of  $I < I_s$ , the Kerr rotation angle  $\theta_K (< \theta_{K,max})$  becomes a current dependent parameter.

b. Ferro/antiferromagnetic exchange-coupled film with a single magnetic domain structure

Since the ferro/antiferro coupling gives rise to an exchange bias magnetic field  $H_{ex}$  in the ferromagnetic layer, the ferromagnetic film has a single magnetic-domain structure. Therefore the ferro/anti-ferromagnetic exchange-coupled film has two advantages for the optical probe current sensor. First, the Barkhausen noise due to the domain wall pinning can be excluded, and the magnetization reversal is dominated only by rotation magnetization when the external magnetic field is applied to the hard magnetization direction (perpendicular to  $H_{ex}$ ). Second, the exchanged-coupled film has an excellent frequency characteristic of magnetic susceptibility  $\chi$ , which is due to additional  $H_{ex}$ . The frequency response is limited by ferromagnetic resonance frequency  $f_r$ . It is easy to obtain higher  $f_r$  over 1 GHz. Since the sensitivity of optical sensor, which is defined as  $\theta_K/I$  in the linear operation region, is proportional to the hard magnetization axis susceptibility  $\chi$ , high speed optical current-sensing can be realized by using the ferro/antiferro coupled film.

The exchange bias field  $H_{ex}$  and the static magnetic susceptibility  $\chi$  in the hard axis of the exchange-coupled film are written as follows [9];

$$H_{ex} = \frac{J_{ex}}{t_F M_s} \quad (1)$$

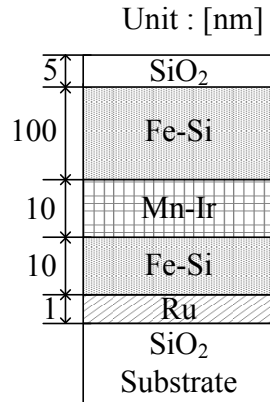


Fig.3 Cross-sectional structure of the Fe-Si/Mn-Ir exchange-coupled magnetic film. The top thin SiO<sub>2</sub> layer is used for avoiding native oxidation of the Fe-Si layer.

$$\chi = \frac{M_s}{H_k + J_{ex}} \quad (2)$$

Where  $J_{ex}$  is the exchange energy,  $t_F$  is the ferromagnetic layer thickness,  $M_s$  is the saturation magnetization and  $H_k$  is the uniaxial anisotropy magnetic field of the ferromagnetic layer. Since the static magnetic susceptibility  $\chi$  can be changed easily by the ferromagnetic layer thickness  $t_F$ , the sensitivity of the optical probe current sensor can be controlled by changing  $t_F$ . In this study, Fe-Si(100 nm)/Mn-Ir(10 nm)/ Fe-Si(10 nm)/Ru(1 nm) was selected for the magnetic film[10].

Fig. 3 shows the cross-sectional structure of the Fe-Si/Mn-Ir exchange couple film. A top 100 nm thick Fe-Si layer with thin passivation layer of SiO<sub>2</sub> operates as the reflective film for the Kerr effect. As described later, a 1312 nm Laser-diode for the optical-fiber communication was used as the light source in the fabricated optical probe current sensor. From the experiment of maximum Kerr rotation angle  $\theta_{K,max}$  by using the magneto-optic measurement set-up (NEOARK: BH- M600VIR-FKR-TU),  $\theta_{K,max}$  was estimated to be about 0.04 degree.  $\theta_{K,max}$  was not so large, therefore a differential detection scheme for the optical signal was introduced to the sensor.

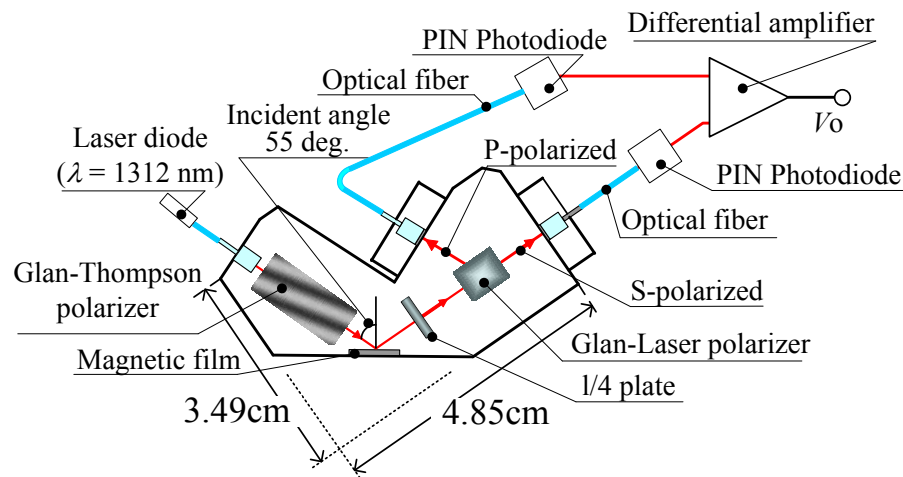
### III. OPTICAL PROBE CURRENT SENSOR MODULE USING THE KERR EFFECT OF EXCHANGE-COUPLED FILM

#### a. Sensor module structure

The Fig. 4 shows a schematic view and a photograph of the optical probe current sensor module. This sensor module consists of a 1312 nm Laser-diode, a polarizer (Glan- Thompson prism), a Fe-Si/ Mn-Ir film, a quarter wavelength plate, a Glan-Laser polarizer, two PIN Photodiodes for

S-polarized and P-polarized light, a differential amplifier and three plastic fibers. The incident angle of linearly polarized light for Fe-Si/Mn-Ir was 55 deg. [10], which gives a maximum Kerr effect. When current  $I = 0$ , linearly polarized reflected light from the top Fe-Si layer is transformed to a circularly-polarized light by quarter wavelength plate, and the principal axis of the quarter-wave plate is adjusted in order to equal the intensity of S-polarized and that of P-polarized light. In case of current flowing (Kerr rotation occurs), the different strength between S-polarized and P-polarized light give rise to an output  $V_o$  through the two PIN Photodiodes and the differential amplifier.

The module size is 3.49 cm X 4.85 cm excluding the Laser-diode, the electronic circuit and the optical fiber.



(a) Schematic view of the optical probe current sensor



(b) Photograph of the optical probe current sensor

Fig. 4 Schematic view and photograph of the optical probe current sensor fabricated. The size is 3.49 cm X 4.85 cm excluding the Laser-diode, the electronic circuit and the optical fiber.

b. A photo signal to electric signal conversion circuit

Fig. 5 shows the photo signal to the electric signal conversion circuit of the optical probe current sensor. Inverse-bias current of the PIN Photodiode, which is proportional to the light intensity, is converted into the voltage across the resistance ( $82\text{ k}\Omega$ ). Since the incident S-polarized and P-polarized light to the PIN Photodiode had a power of  $120\text{ }\mu\text{W}$  in case of current  $I = 0$ , each dc-offset voltage of  $82\text{ k}\Omega$  resistance was adjusted to zero in the next-stage inverting amplifier. In the final-stage differential amplifier, an output voltage  $V_o$  was proportional to the difference of the change of P-polarized and S-polarized light due to Kerr rotation.

The frequency bandwidth of the PIN photodiode circuit depends on the product of parasitic capacitance and external resistance. The fabricated PIN Photodiode circuit had the bandwidth of  $1.2\text{ MHz}$ . The designed total voltage-gain through the inverting amplifier and the differential amplifier was  $100$  ( $40\text{ dB}$ ) with  $-3\text{ dB}$  bandwidth of  $200\text{ kHz}$ . Fig. 6 shows the gain *v.s.* frequency. A measured gain was about  $41\text{ dB}$  and cut-off frequency was about  $200\text{ kHz}$ . The sensor output

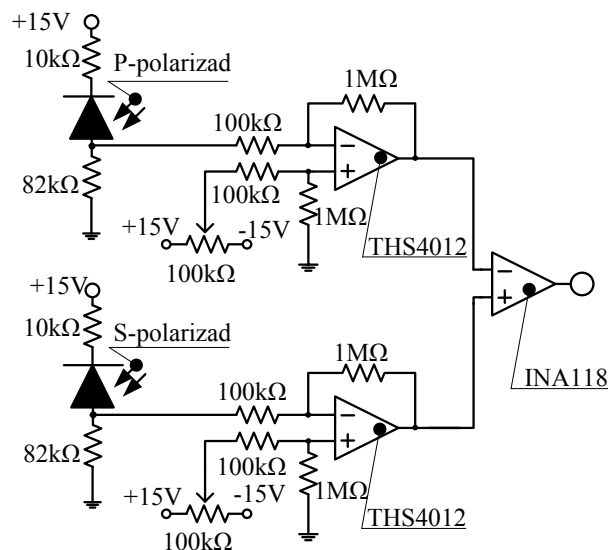


Fig. 5 Photo signal to electric signal conversion circuit.

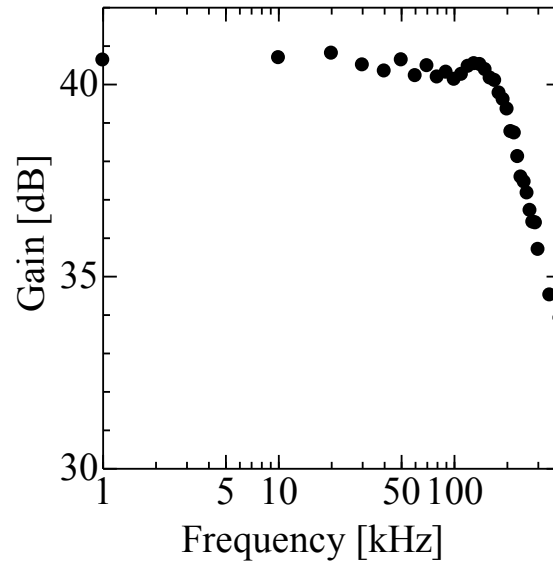


Fig. 6 Gain *v.s.* frequency characteristic through the inverting amplifier and differential amplifier.

noise at zero-current condition was  $\pm 100$  mV, and it was considered that the main reason for this may be owing to the small Kerr rotation angle of Fe-Si, and lesser reason might be the dark current noise of the PIN Photodiode and the circuit noise.

### c. Basic experiment for the fabricated sensor module

Fig. 7 shows a basic experimental set-up for the fabricated sensor module. As the ac magnetic field generation apparatus, a 1150 turn-solenoid coil was used, and the fabricated sensor module was set in the center of the solenoid coil. Fig. 8 shows the relationship between the sensor output *v.s.* the ampere-turn of the solenoid coil. The normalized magnetization curve of the upper 100 nm thick Fe-Si layer of the Fe-Si/ Mn-Ir film is also shown in this figure. Sensor output *v.s.* ampere-turn corresponds well to the magnetization curve. From the experimental results, it was found that the sensor output is approximately proportional to the external field  $H$  ranging from -20 to 20 Oe.

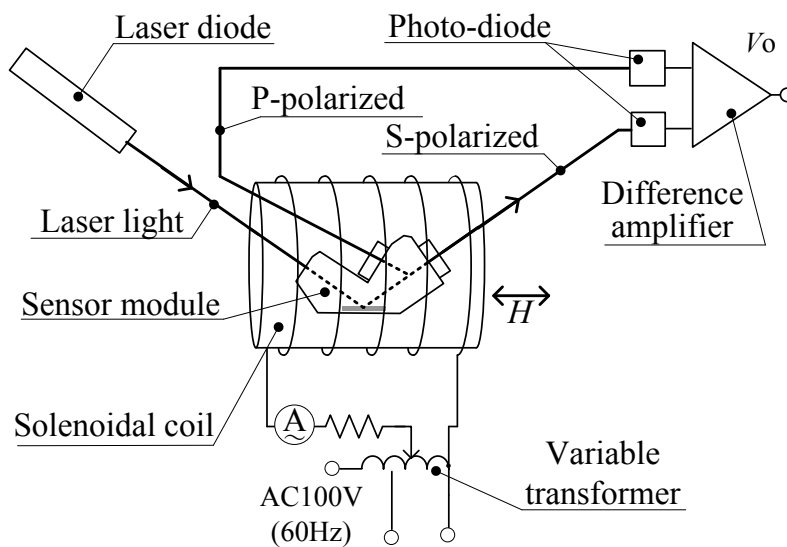


Fig. 7 Basic experimental set-up for the sensor module.

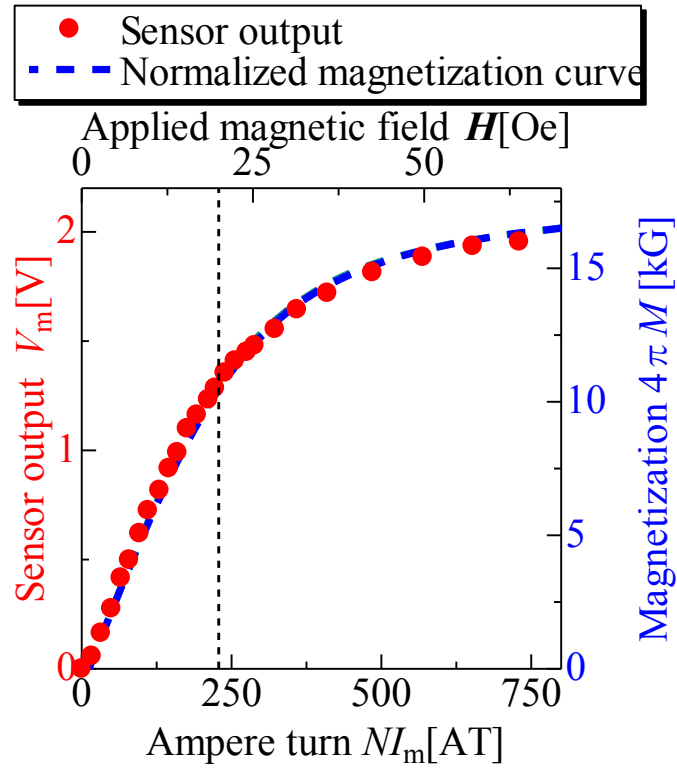


Fig. 8 Relationship between the sensor output and the ampere-turn of the 1150 turn-solenoid coil. Normalized magnetization curve of the upper 100 nm thick the Fe-Si layer of Fe-Si/Mn-Ir film is also shown.

#### IV. SWITCHING CURRENT MEASUREMENT OF THE IGBT

##### a. Experimental set-up

Fig. 9 shows the experimental circuit of the IGBT switching current measurement using the optical probe current sensor. The dc voltage  $V_d$  generated using a double-voltage rectifier circuit was 340 V. The high and low-side IGBT switches (CM200DU-24NFH; Mitsubishi Electric Co.) were used. The reactor  $L$  with 1 mH inductance was connected in parallel to the high-side switch. The high-side switch was turned-off at all times, and the low-side switch was turned-on and off repetitively.

In this experiment, the turn-on time was 50  $\mu$ s and turn-off time was 150  $\mu$ s. Fig.10 shows the schematic view of the current flowing when low-side IGBT turned-on or off. When the low-side switch is turned-on, the current flows through the reactor and the low-side switch, and it increases proportionally with time (magnetic energy storage period) (Fig.10(a)). On the other hand, when the low-side switch is turned-off, the circulating current flows through the reactor and the body-diode of the high-side switch (Fig.10(b)). Under ideal conditions, the low-side IGBT current  $i_L$  in the turn-on period can be expressed as follows;

$$i_L = \frac{V_d}{L} t_{\text{on}} \quad (3)$$

Here  $V_d$  is the dc voltage (340 V), and  $L$  is the inductance of the reactor (1 mH). In case of the turn-on period of 50  $\mu$ s, the current  $i$  increases up to 17 A. When the low-side IGBT is turned-off at  $t > 50 \mu$ s, the circulating current through the reactor and the body diode of the high-side IGBT would be kept to 17 A in 150  $\mu$ s period because of small series-resistance in the reactor and body diode. When the low-side IGBT is turned-on again at  $t = 200 \mu$ s, the current  $i_L$  would increase according to the following equation;

$$i_L = 17 + \frac{V_d}{L} t_{\text{on}} \quad (4)$$

At  $t = 250 \mu$ s, the current is  $i_L$  34 A. In this experiment, the low-side switch was turned on and off repetitively four times. Therefore, at  $t = 650 \mu$ s, the current is  $i_L$  68 A.

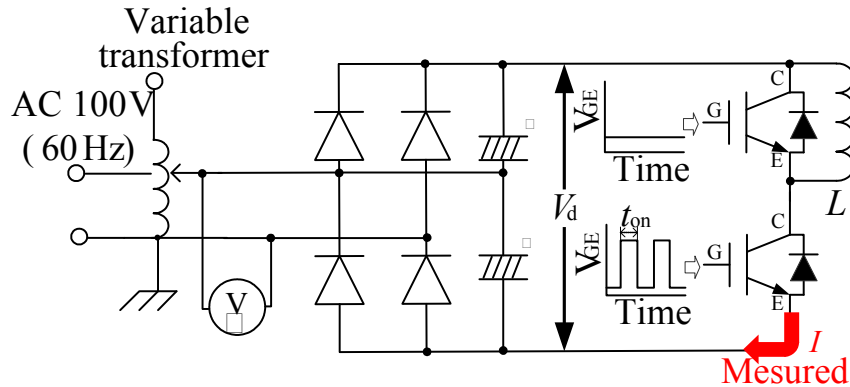


Fig. 9 Experimental circuit of IGBT switching current measurement using optical probe current sensor module.

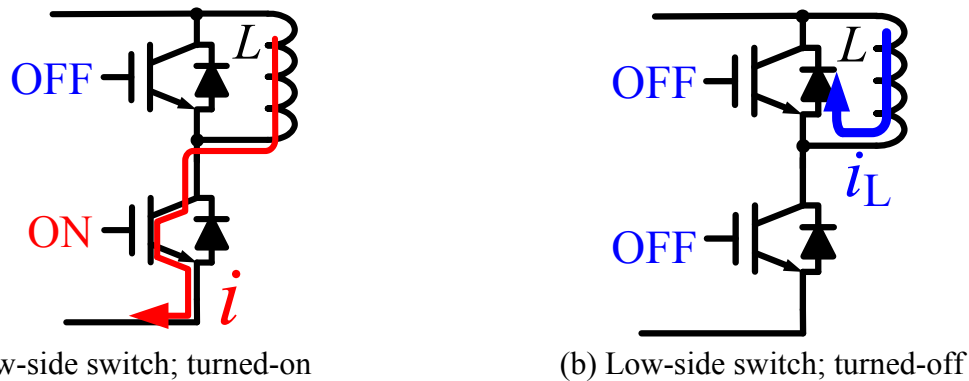


Fig. 10 Schematic view of current flowing when low-side IGBT turned on or off

## b. IGBT switching current measurement

By using the experimental circuit shown in Fig. 9, the switching current of low-side IGBT was measured by the fabricated optical probe current sensor module. The magnetic yoke for increasing sensor sensitivity was not used in this experiment, and the fabricated sensor module was put directly on an aluminum bus-bar.

Fig.11 shows the low-side IGBT current waveform measured by the optical probe current sensor. The dc voltage  $V_d$  was 340 V, the quad gate-pulse was applied to the low-side IGBT, the turn-on period of low-side IGBT was 50  $\mu\text{s}$  and turn-off period of it was 150  $\mu\text{s}$  (25 % duty). The results are: the first, the second, the third and the fourth peak current were estimated to be about 14, 27, 41 and 61 A respectively.

Fig.12 shows the measured sensor output voltage v.s. current flowing through the bus bar. It was found that the sensor output is approximately proportional to current flowing through the bus bar ranging from 0 to 60 A. However, the measured peak currents were lower than the predicted

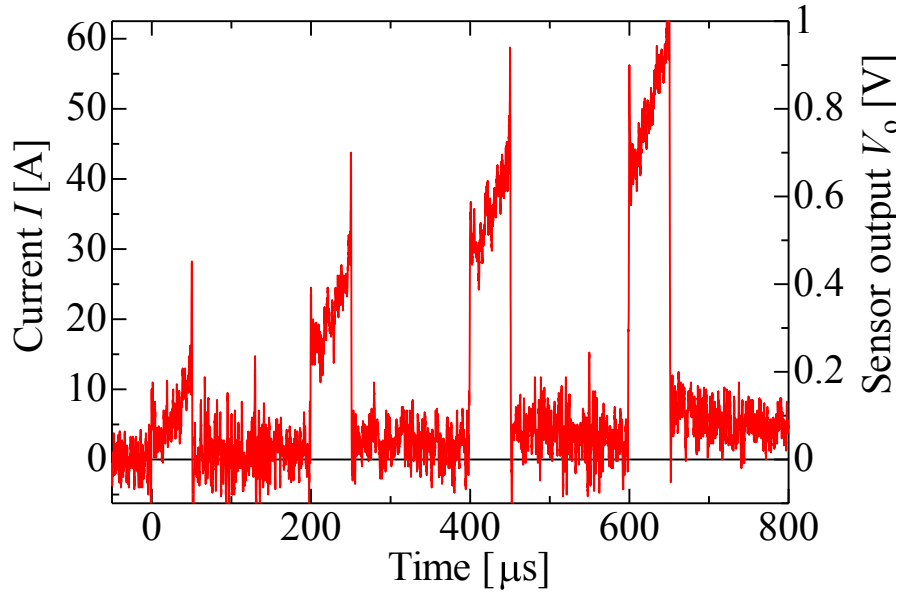


Fig. 11 Switching current waveform measured using the fabricated optical probe current sensor module.

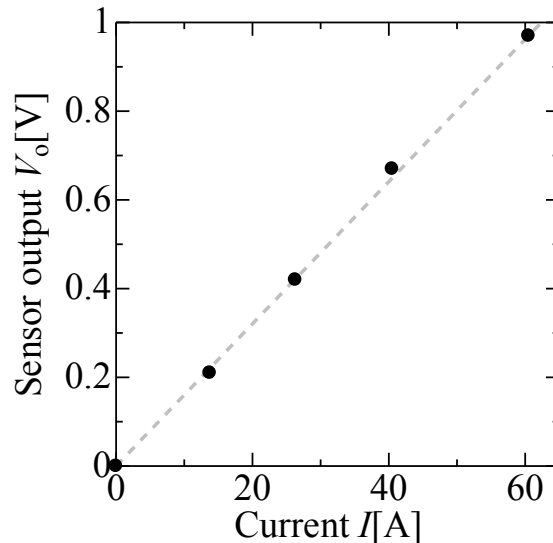


Fig. 12 Measured sensor output voltage *v.s.* Current flowing through the bus bar values of 17, 34, 51 and 68 A. It was considered that the series resistance of the reactor and on-resistance of the IGBT caused the voltage drop.

In the turn-off period of the low-side IGBT, the sensor output was not zero (undesirable off-set). This is owing to the stray magnetic field generated by the circulating current through the reactor (Fig.10(b)) because the sensor has no magnetic yoke for suppressing the stray field. Such undesirable off-set will be suppressed using magnetic shield techniques.

## V. CONCLUSIONS

This paper describes an optical probe current sensor module using the Kerr effect and its application to IGBT switching current measurement. By using a single magnetic-domain Fe-Si/Mn-Ir exchange-coupled film, the Barkhausen noise due to domain wall pinning can be excluded, and high-sensitivity in current measurements are realized using differential detection. The sensor-head has a compact size of 3.49 cm X 4.85 cm. By using the sensor module, 60 A IGBT switching current measurement has been demonstrated. In the future, a mm-scale miniature sensor module will be developed for application to the PCU of HV/HEV.

## ACKNOWLEDGMENT

We would like to thank Prof. M. Inoue and Mr. S. Baek of Toyohashi Technological University, Toyohashi, Japan, of the Kerr effect measurement for the Fe-Si/Mn-Ir film.

## REFERENCES

- [1] T. Ishikawa, H. Sugiyama, R. Oka, Y. Suzuki, E. Baba, Y. Kawase, M. Tatsuno, "Reactor Vibration Analysis in Consideration of Coupling between the Magnetic Field and Vibration", IEEE Industry Applications Conference, October 2004
- [2] H. Kim, G. Kang, D. Nam "Coreless Hall Current Sensor for Automotive Inverters Decoupling Cross-coupled Field", Journal of Power Electronics, Vol.9, No.1, January 2009. pp. 68-73
- [3] M. Imamura, M. Nakahara, and S. Tamura, "Output Characteristics of Field Sensor Used for Optical Current Transformers Applied to the Flat-Shape Three-Phase Bus-Bar", IEEE Transactions on Magnetics, Vol.33, No.5, September 1997, pp.3403-3405
- [4] M. Iwanami, M. Nakada, H. Tsuda, K. Ohashi, and J. Akedo : "Ultra small magneto-optic field probe fabricated by aerosol deposition", IEICE Electronics Express, Vol.4, No.17, September 2007, pp.542-548

- [5] E. Yamazaki, S. Wakana, H. Park, M. Kishi, M. Tsuchiya, "High-Frequency Magneto-Optic Probe Based on BiRIG Rotation Magnetization", *IEICE Transactions on Electronics*, Vol.E86-C, No.7, July 2003, pp. 1338-1344.
- [6] K. Kurosawa, K. Yamashita, T. Sowa, Y. Yamada, "Flexible Fiber Faraday Effect Current Sensor Using Flint Glass Fiber and Reflection Scheme", *IEICE Transactions on Electronics*, Vol.E83-C, No.3, March 2000, pp. 326-330
- [7] R. Carey and E. D. Isaac, "Magnetic Domains and Techniques for Their observation", Academic Press, 1966, pp.62-80
- [8] M. Sonehara, T. Sugiyama, T. Sato, K. Yamasawa, Y. Miura, "Preparation and Characterization of Mn-Ir/Fe-Si Exchange-Coupled Multilayer Film with Ru Underlayer for High-Frequency Applications", *IEEE Transactions on Magnetics*, Vol.41, No.10, October 2005, pp.3511-3513
- [9] M. Jimbo, "Present status of antiferromagnetic materials in spin valves", *Journal of the Magnetics Society of Japan*, Vol.22, No.1, 1988, pp12-18
- [10] M. Sonehara, K. Asanuma, N. Otani, T. Goto, Y. Kikuchi, T. Sato, K. Yamasawa, Y. Miura "Fundamental Study of Optical Probe Current Sensor using Kerr Effect of Single Magnetic Domain Film", *IEEE Sensors 2009 Conference*, October 2009, pp.1232-1237